Synthesis, characterization and magnetic evaluation of praseodymium modified cerium oxide

A F Cruz Pacheco[1], J A Gómez Cuaspud[1] and C A Parra Vargas[1]
[1] Universidad Pedagógica y Tecnológica de Colombia, Tunja, Colombia

E-mail: andresfelipe.cruz@uptc.edu.co

Abstract. This paper report the synthesis, characterization and magnetic evaluation of $Ce_{0.6}Pr_{0.4}O_2$ system using a chemical route that involves the combustion of citrate species. The precursors were characterized by Fourier transform infrared spectroscopy (FTIR), to identify, the main vibrational bands associated with the organic material after combustion process. The structural analysis by X-ray diffraction (XRD) revealed the obtaining of an Fm-3m (225) cubic phase with a particle size around 10nm. Finally, the measurement of the magnetization as a function of applied magnetic field and of susceptibility showed a perfect paramagnetic behaviour.

1. Introduction

With the progress of technology, there are new challenges for the development of advanced ceramic materials, in which the rare earth elements have shown unusual and interesting properties for a wide application field. In this context, the cerium is particularly one of the most important and abundant elements in nature and just as praseodymium are the only elements of this group that are stable in two oxidation states Ce^{4+}, Ce^{3+}, Pr^{4+} and Pr^{3+}. The CeO_2 and Pr_6O_{11}, are the most common oxides of these elements and their importance focuses on the possibility to participate in redox reactions and the storage capacity and controlled release of oxygen through the conversion between the main oxidation states respectively. The oxygen vacancies that arise from this conversion can be chemically manipulated by the combination of the two compounds originating materials with electronic, structural, mechanical, optical, catalytic and magnetic properties for technological applications. Some of the most important properties of these oxides have focused on the field of catalysis and photocatalysis [1,2], in development of oxygen sensors and biomaterials [3,4], and design of components for solid oxide fuel cells SOFC [5,6]. Commonly these materials are prepared by solid state reaction, however the low homogeneity of products and the restricted kinetic associated with the synthesis process and the loss of textural, surface and morphological properties, make the current trend is to use alternative routes leading to a better control of composition, structure and purity of phase at nanometric scale. In this sense, the combustion method is one of the most viable for its simplicity, speed and economy, reason why, present work pretend to show the advantage of combustion process in the obtaining of nanostructured oxides based on $Ce_{0.6}Pr_{0.4}O_2$ system [7–9].

2. Experimental

Stoichiometric amounts of $Ce(NO_3)_3.6H_2O$ (99.9%), $Pr(NO_3)_3.6H_2O$ (99.9%) and citric acid monohydrated (99.9%) were used in the preparation of the $Ce_{0.6}Pr_{0.4}O_2$ system, by the combustion method. The oxide was synthesized starting from solutions of nitrates of Ce^{3+} and Pr^{3+}, (Previously

Content from this work may be used under the terms of the Creative Commons Attribution 3.0 licence. Any further distribution of this work must maintain attribution to the author(s) and the title of the work, journal citation and DOI.
Published under licence by IOP Publishing Ltd

validated [10]), using a glass reactor equipped with magnetic stirring (150rpm), temperature control and reflux, as described elsewhere [11]. Once adjusted the corresponding dissolutions, the citric acid was added in a molar ratio 1:0.5, with respect to the total concentration of cations. The system was kept under reflux at 140°C for 12 hours until formation of a viscous liquid, which was then heated at 200°C under air flux in an oven until complete solvent evaporation and treated at 310ºC to initiate the combustion process. The precursor formed was treated at 500°C to remove the remaining carbon under oxygen flow for 2 hours.

The metal-organic precursor was analysed by infrared spectroscopy FTIR, using a Shimadzu FTIR prestige-21 equipment in ATR configuration (attenuated total reflectance), in order to assess the formation of citrate complexes and allow the verification of the effectiveness of the synthesis process and the chemical composition. The crystalline structure of the solid after calcination of precursor, was evaluated by X-ray diffraction (XRD), on a PANalytical X'Pert PRO MPD diffractometer, equipped with Ultra-Fast X´celerator detector and Bragg-Brentano configuration, using Cu Kα radiation (λ=1.54186Å) between 20º and 90°. The measurements were developed with a voltage of 40kV and a current of 20 mA in all cases. The crystallite size was calculated using the highest diffraction signals by the Debye-Scherrer equation, taking the value of half peak width set by a Lorentzian function and using a constant of 0.89 as reference [12]. The magnetization hysteresis (M-H) loop and zero field cooling (ZFC) studies, of the $Ce_{0.6}Pr_{0.4}O_2$ system, was carried out by using a vibrating sample magnetometer VersaLab (VSM). The magnetization measurements were performed at several magnetic fields (500Oe–5000Oe), and the magnetic hysteresis measurements were done at different temperatures (100 and 300K) [13].

3. Results and discussion

FTIR spectrum of the $Ce_{0.6}Pr_{0.4}O_2$ precursor before and after combustion process is shown in Figure 1.

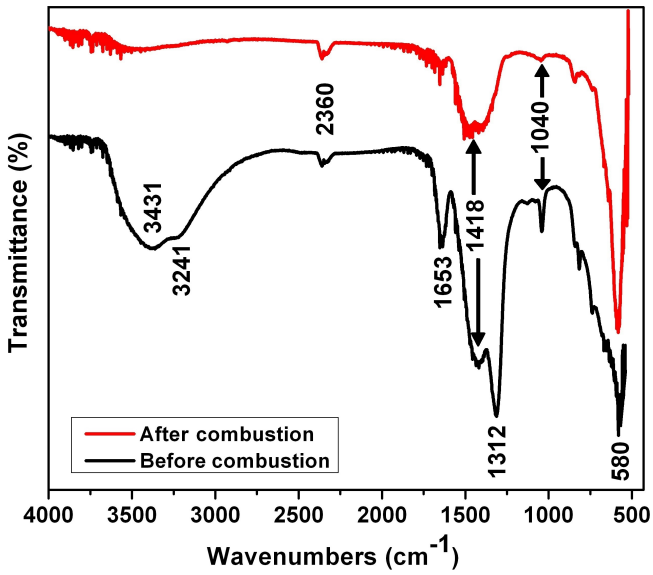


Figure 1. Infrared spectrum of the $Ce_{0.6}Pr_{0.4}O_2$ precursor before and after the combustion process.

The spectrum of precursor before combustion process, shown characteristic absorption bands associated with a polymeric citrate complex, which confirms the formation of coordination compounds between metals and citrate species as reported previously by Wahba [14]. The intense absorption band at 3431cm^{-1} is attributed for (O-H) vibration modes of the water molecules coordinated to the complex. The band stretching at 3241cm^{-1} is assigned for vibrational mode of (N-H) bond, which is associated with the addition of ammonia to dissolution for pH adjustment. The weak

band observed at 2360cm^{-1} is associated with the presence of CO_2, which it is occluded in the materials during the synthesis [15]. The band located at 1653cm^{-1} is related with the asymmetric deformation mode of carboxyl group of mono-dentate coordination compounds and the bands attributed the symmetric stretching at 1418 and 1312cm^{-1} for the respective (COOH) groups, corresponds to a strong stretch mode associated to bidentate coordination compounds [16,17].

The absorption bands observed at 1041cm^{-1} corresponds the stretching modes of the (CO) bonding associated with acetals and primary alcohols, as well as bends out of plane of (C-H) bond [18]. The absorption peaks in the region 900–500cm^{-1} are associated with the bond of the metal cations with oxygen atoms. The characteristic band at around 580cm^{-1} is assigned for the symmetric stretching vibration of Ce-O-Ce, Ce-O-Pr or Pr-O-Pr [19–21]. While, there is still presence of absorption bands related to symmetrical and asymmetrical deformations of the groups (COOH) and a band to lower frequencies corresponding to the vibrational modes of the links C-O associated acetals and primary aliphatic alcohols. So, the intense band at 580cm^{-1}, indicate that the cerium and praseodymium cations are tightly bound with oxygen [22], which implies that synthesis process has a significant decrease in terms of time and efficiency.

Structural identification of $Ce_{0.6}Pr_{0.4}O_2$ system was determined using XRD as shown in Figure 2. XRD patterns reveal the formation of a single phase with cubic structure type fluorite and space group Fm-3m (225) with a lattice constant a=0.5411nm, according with the reference compound of CeO_2, ICDD code 00-034-0394.

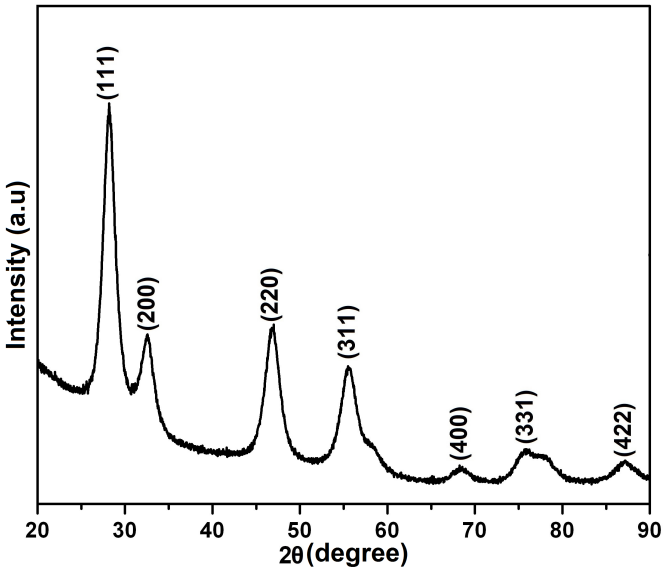


Figure 2. X-ray diffraction pattern of $Ce_{0.6}Pr_{0.4}O_2$ system.

According to XRD data, the crystallite size (D) was to be about 10 nm and was calculated using the Scherrer formula:

$$D = \frac{0.89\lambda}{\beta cos\theta} \quad (1)$$

Where λ was the X-ray wavelength, β was the width of the peak highest intensity considered in the calculation and θ was the Bragg diffraction angle of the main reflection (1 1 1) [23].

The broadening of the peaks is due to the incorporation of Pr to cerium oxide structure, which leads to an increase in the solids density and heterogeneity in the structural composition at nanoscopic level [24]. These phenomena are due to the ionic radius of Pr^{3+} (1.126Å), which is much larger than Ce^{4+} and Ce^{3+} (1.034Å) cations. However, the Pr^{4+} (0.96Å) radius is slightly smaller than that for Ce^{4+} (0.97Å)

[25–27], therefore the difference of ionic radius cause a change in the Ce–O bond length and in the crystal size of the sample [28].

Figure 3 shows the experimental data of the magnetization (M), as a function of applied magnetic field (H) for $Ce_{0.6}Pr_{0.4}O_2$ system measured at 100 and 300K. The sample exhibits a perfect paramagnetic behaviour at 100 and 300 K since the magnetization is reversible and has a linear curve.

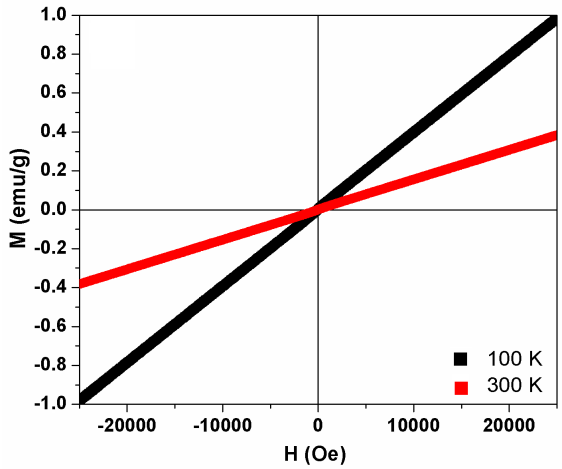


Figure 3. Magnetization (M) of $Ce_{0.6}Pr_{0.4}O_2$ system as a function of the applied magnetic field (H) at 100 and 300K.

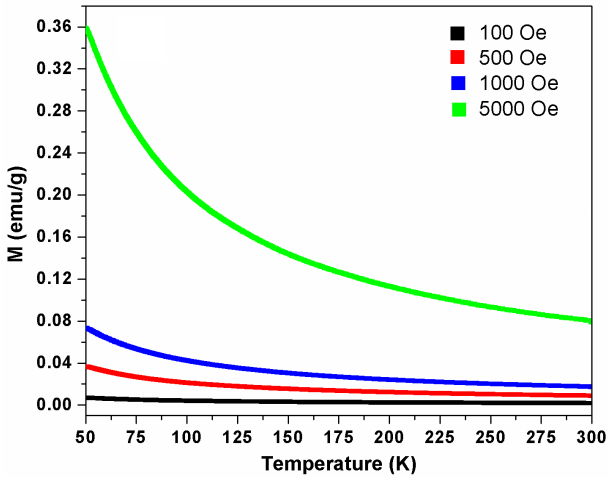


Figure 4. Magnetic susceptibility as a function of temperature for $Ce_{0.6}Pr_{0.4}O_2$ in the magnetic fields 100, 500, 1000 and 5000Oe.

The temperature dependence of the magnetic susceptibility for $Ce_{0.6}Pr_{0.4}O_2$ was performed at four magnetic fields (100, 500, 1000 and 5000Oe) as shown in Figure 4. All ZFC curves present a paramagnetic behaviour, with increased susceptibility when a temperature decreases. The behaviour that presents the sample is due to the incorporation of praseodymium in the fluorite structure of cerium oxide. The Pr^{4+} and Pr^{3+} ions have net magnetic moments that make them paramagnetic [29]. In the same way, the paramagnetic component also comes from the Ce^{3+} ions due to the one unpaired electron in a 4*f* orbital [30]. Furthermore, the diamagnetic behaviour of Ce^{4+} ions not present in measures magnetization vs applied field and the ZFC curves, so is at low proportion [31].

4. Conclusions

The $Ce_{0.6}Pr_{0.4}O_2$ system, was prepared by the combustion method, obtaining material at the nanometric order. The FT-IR analysis of metal-organic precursors, allowed evaluate the main absorption bands related with the formation of polymeric complexes between metal cations and citrate species. The structural characterization evaluated by X-ray diffraction, confirms obtaining an oxide with structure fluorite type according to the reference compound. The crystal size of sample was 10nm, using the Debye–Scherrer equation. The magnetic response produced by $Ce_{0.6}Pr_{0.4}O_2$ system was attributed to paramagnetic behaviour due to Ce^{3+}, Pr^{3+} y Pr^{4+} ions have a net magnetic moment.

References

[1] Nakagawa K, Ohshima T, Tezuka Y, Katayama M, Katoh M and Sugiyama S 2015 *Catal. Today* **246** 67
[2] Contreras-García M E, García-Benjume M L, Macías-Andrés V I, Barajas-Ledesma E, Medina-Flores A and Espitia-Cabrera M I 2014 *Mater. Sci. Eng. B* **183** 78
[3] Chen C Y, Chang K H, Chiang H Y and Shih S J 2014 *Sensors Actuators B Chem.* **204** 31
[4] Kolli M B, Manne N D P K, Para R, Nalabotu S K, Nandyala G, Shokuhfar T, He K, Hamlekhan A, Ma J Y, Wehner P S, Dornon L, Arvapalli R, Rice K M and Blough E R 2014 *Biomaterials* **35** 9951
[5] Taguchi H, Chiba R, Komatsu T, Orui H, Watanabe K and Hayashi K 2013 *J. Power Sources* **241** 768
[6] Stojadinović B, Dohčević-Mitrović Z, Paunović N, Ilić N, Tasić N, Petronijević I, Popović D and

Stojanović B 2016 *J. Alloys Compd.* **657** 866
[7] Chen B, Rao G, Wang S, Lan Y, Pan L and Zhang X 2015 *Mater. Lett.* **154** 160
[8] Deganello F, Marcì G and Deganello G 2009 *J. Eur. Ceram. Soc.* **29** 439
[9] Rajpure K Y 2015 *Superlattices Microstruct.* **77** 181
[10] Gómez-Cuaspud J A and Valencia-Ríos J S 2009 *Rev. Colomb. Química* **38** 289
[11] Rodrigues C P and Schmal M 2011 *Int. J. Hydrogen Energy* **36** 10709
[12] Mustafa G, Islam M U, Zhang W, Jamil Y, Asif Iqbal M, Hussain M and Ahmad M 2015 *J. Magn. Magn. Mater.* **378** 409
[13] Mejía-Gómez J A, Supelano-García I, Palacio C A and Parra-Vargas C A 2015 *J. Phys. Conf. Ser.* **614** 012003
[14] Wahba A M, Aboulfotoh-Ali N and Eltabey M M 2014 *Mater. Chem. Phys.* **146** 224
[15] Gómez-Cuaspud J A, Valencia-Ríos J S and Carda-Castelló J B 2010 *J. Chil. Chem. Soc.* **55** 445
[16] Chen Y and Xiao J Z 2013 *Ceram. Int.* **39** 9599
[17] Shaikh P A, Kambale R C, Rao A V and Kolekar Y D 2010 *J. Alloys Compd.* **492** 590
[18] da Silva M F P, de Souza-Carvalho F M, da Silva-Martins T, de Abreu-Fantini M C and Isolani P C 2010 *J. Therm. Anal. Calorim.* **99** 385
[19] Vanhoyland G, Pagnaer J, D'Haen J, Mullens S and Mullens J 2005 *J. Solid State Chem.* **178** 166
[20] Yang W D, Chang Y H and Huang S H 2005 *J. Eur. Ceram. Soc.* **25** 3611
[21] Esther Jeyanthi C, Siddheswaran R, Kumar P, Siva Shankar V and Rajarajan K 2014 *Ceram. Int.* **40** 8599
[22] Ho C, Jimmy Y, Kwong T, Mak A C and Sukyin L 2005 *Chem. Mater.* **17** 4514
[23] Li X, Feng Z, Lu J, Wang F, Xue M and Shao G 2012 *Ceram. Int.* **38** 3203
[24] Gerasimov E Y, Isupova L A and Tsybulya S V 2015 *Mater. Res. Bull.* **70** 291
[25] Matovic B, Boskovic S, Logar M, Radovic M, Dohcevic-Mitrovic Z, Popovic Z V and Aldinger F 2010 *J. Alloys Compd.* **505** 235
[26] Shannon R D 1976 *Acta Crystallogr. Sect. A* **32** 751
[27] Chiba R, Taguchi H, Komatsu T, Orui H, Nozawa K and Arai H 2011 *Solid State Ionics* **197** 42
[28] Phokha S, Prabhakaran D, Boothroyd A, Pinitsoontorn S and Maensiri S 2014 *Microelectron. Eng.* **126** 93
[29] Kern S 1964 *J. Chem. Phys.* **40** 208
[30] Niu G, Hildebrandt E, Schubert M A, Boscherini F, Zoellner M H, Alff L, Walczyk D, Zaumseil P, Costina I, Wilkens H and Schroeder T 2014 *ACS Appl. Mater. Interfaces* **6** 17496
[31] Bernardi M I B, Mesquita A, Béron F, Pirota K R, de Zevallos A O, Doriguetto A C and de Carvalho H B 2015 *Phys. Chem. Chem. Phys.* **17** 307